INTERNATIONAL JOURNAL OF REFRIGERATION 34 (2011) 1898–1910

available at www.sciencedirect.com

journal homepage: www.elsevier.com/locate/ijrefrig

Impact of classical assumptions in modelling a microchannel gas cooler

Santiago Martínez-Ballester [a,*], *José-M. Corberán* [a], *José Gonzálvez-Maciá* [a], *Piotr A. Domanski* [b]

[a] *Instituto de Ingeniería Energética, Universidad Politécnica de Valencia, Camino de Vera s/n, Valencia 46022, Spain*
[b] *HVAC&R Equipment Performance Group, National Institute of Standards and Technology, Gaithersburg, MD 20899, USA*

ARTICLE INFO

Article history:
Received 4 January 2011
Received in revised form
18 July 2011
Accepted 19 July 2011
Available online 27 July 2011

Keywords:
Heat exchanger
Modelling
Simulation
Microchannel
Fin
Gas cooler

ABSTRACT

Most of the current air-to-refrigerant heat exchanger models use the classic ε-NTU approach, or some of its assumptions. These models do not account for longitudinal heat conduction in the tube and the fin, and the heat conduction between different tubes. This paper presents a more fundamental numerical approach to heat exchanger modelling which takes into account the 2D longitudinal heat conduction in any element, does not apply the fin theory, and captures a more detailed representation of air properties. Using the fundamental numerical approach, the paper assesses the impact of the traditional heat exchanger model assumptions when modelling a microchannel gas cooler working with CO_2. The study revealed significant differences in capacity predictions depending on the ε-NTU relationship adopted. Large errors in capacity prediction of individual tubes occurred due to the adiabatic-fin-tip assumption when the neighbouring tubes were of different temperature.

Impact des hypothèses classiques sur la modélisation d'un refroidisseur de gaz à microcanaux

Mots clés : Échangeur de chaleur ; Modélisation ; Simulation ; Microcanal ; Ailette ; Refroidisseur de gaz

1. Introduction

The use of microchannel heat exchangers is increasing because of their compactness and high effectiveness. In the case of transcritical CO_2 systems, microchannels have an additional merit related to their high mechanical strength. As with other products, reliable simulation models can provide substantial cost savings during the design and optimization process of heat exchangers. Currently, several models or simulation tools for heat exchanger are available in the literature: for finned tubes (Lee and Domanski, 1997; Corberán et al., 2002; EVAP-COND, 2003; Jiang et al., 2006; Singh et al., 2008) and microchannel heat exchangers (Yin et al., 2001; Jiang et al., 2006; Shao et al., 2009; Fronk and Garimella,

* *Corresponding author*. Tel.: +34 963 879 121; fax: +34 963 879 126.
E-mail address: sanmarba@iie.upv.es (S. Martínez-Ballester).
0140-7007/$ – see front matter © 2011 Elsevier Ltd and IIR. All rights reserved.
doi:10.1016/j.ijrefrig.2011.07.005

Nomenclature

A	heat transfer area (m^2)
a,b,c,d,e	grid dimensions
BU	both unmixed: air and refrigerant
c_p	specific heat ($J\ kg^{-1}\ K^{-1}$)
D	tube depth (m)
G	mass flux ($kg\ m^{-2}\ s^{-1}$)
H	fin height (m)
h	specific enthalpy ($J\ kg^{-1}$)
Hp	tube pitch (m)
k	thermal conductivity ($W\ m^{-1}\ K^{-1}$)
L	tube length (m)
l	distance between two wall cells (m)
LHC	longitudinal heat conduction
$\dot{m}$	mass flow rate ($kg\ s^{-1}$)
N	number of cells
NTU	number of transfer units
P	wetted perimeter (m)
$\dot{q}$	heat flux ($W\ m^{-2}$)
RMAU	refrigerant mixed and air unmixed
s	length in the forward direction of a fluid
T	temperature (K)
t	thickness (m)
U	overall heat transfer coefficient ($W\ m^{-2}\ K^{-1}$)
X,Y,Z	spatial coordinates (m)

Greek symbols

α	convective heat transfer coefficient ($W\ m^{-2}\ K^{-1}$)
ε	heat exchanger effectiveness

Subscript

air	air
i	fluid cell index
in	inlet
j	wall cell index
k	direction index
N,S,W,E,J	directions of neighbour wall cell
out	outlet
w	wall
X,Y,Z	spatial directions

2011; García-Cascales et al., 2010). Some of them (Yin et al., 2001; Corberán et al., 2002; Singh et al., 2008; Shao et al., 2009) apply energy conservation equations to each control volume, while others (EVAP-COND, 2003; Jiang et al., 2006; Fronk and Garimella, 2011; García-Cascales et al., 2010) apply directly the solution given by the ε-NTU methodology. The main difference between both methodologies is that the ε-NTU model uses several implicit assumptions resulting in less freedom to describe the actual processes. However, the models based on energy conservation equations usually apply the same assumptions made in ε-NTU approaches. These classical assumptions are the following:

- Steady state.
- Uniform fluid properties.
- Use of fin efficiency.
- Adiabatic-fin-tip assumption for the fin efficiency evaluation.
- One-dimensional heat conduction.

Steady state is a real assumption, which is satisfied. The fluid properties issue is easily addressed by splitting the heat exchanger into segments. On the other hand, not using the ε-NTU methodology has the disadvantage of losing an accurate fluid temperature function, which requires assuming some temperature profile for the fluids. This problem can be solved by dividing the heat exchanger into smaller segments, which improves the representation of non-uniform air and refrigerant properties. In most published models, this methodology improves only the representation of the refrigerant properties because no discretization is provided in the air flow direction. This leads to approximated air properties for the heat exchanger depth (air flow path) based on the average of the inlet and outlet temperatures.

The fin efficiency is calculated following the fin theory, which is developed assuming uniform air temperature along the fin height and uniform heat transfer coefficients. The assumption of uniform air temperature along the fin height is violated since there is a temperature variation along the fin height, as can be expected for the air close to the tube walls.

The ε-NTU methodology needs the use of fin efficiency. To the knowledge of the authors, all models available in the literature, which use a finite volume method (FVM) (Patankar, 1980), apply the fin efficiency with the adiabatic-fin-tip. This efficiency, fundamentally, does not lend itself to accounting for heat transfer via fins between tubes of different temperatures. Several experimental studies indicated that the heat exchanger performance can be significantly degraded by the tube-to-tube heat transfer via connecting fins. For example, Domanski et al. (2007) measured as much as 23% reduction in finned-tube evaporator capacity when different exit superheats were imposed on individual refrigerant circuits. Park and Hrnjak (2007) reported a 3.9% capacity improvement in a microchannel CO_2 gas cooler after introducing fin cuts between selected tubes. Also Zilio et al. (2007) concluded that heat conduction through fins in a CO_2 gas cooler had a significant impact on the capacity. In fact, cut fin surfaces are increasingly being used in heat exchangers to reduce the heat conduction between tubes and improve the heat exchanger performance.

Many authors use different approaches to introduce the heat conduction between tubes in their models. Singh et al. (2008) presented a model, referred to as a "resistance model", to account for heat transfer between tubes through the fins in finned-tube heat exchangers using a segment-by-segment approach. Instead of using the ε-NTU approach, they applied energy equations to each segment and included a term for heat conduction through fins between neighbouring tubes while still using the concept of adiabatic-fin-tip efficiency. The authors explained that the use of a set of energy conservation equations is better than the use of ε-NTU methodology with the included heat conduction term because the ε-NTU relationship assumes all heat is transferred from one fluid to another without internal heat transfer within the

heat exchanger wall structure itself. Their validation effort showed improved model predictions when heat conduction effects were included: predicted heat load agreement within ±3% of the experimental data instead of ±5% corresponding to the model without heat conduction between tubes; the temperature distribution prediction showed an agreement within ±3.3 °C of the experimental data instead of ±8.5 °C corresponding to the model without heat conduction between tubes. Asinari et al. (2004) proposed a three-dimensional model for microchannel gas coolers using CO_2 as refrigerant. This model discretizes the equations by means of a finite volume and finite-element hybrid technique taking into account longitudinal heat conduction (LHC) along all directions for all elements (fins and tubes), thus it does not employ the adiabatic-fin-tip assumption. They investigated the impact of longitudinal heat conduction effects on capacity, and also studied the prediction error due to the adiabatic-fin-tip assumption. The authors concluded that when tube temperatures are different, the use of the adiabatic-fin-tip efficiency gives accurate predictions of the total heat capacity although it does not accurately represent the actual distribution of heat flow between the fin roots. But they did not report the effects in the predicted capacity for the individual tubes of the heat exchanger. It has to be noted that a consequence of a wrong prediction of the individual tube capacity introduces a wrong evaluation of the fluid properties at the tube outlet section.

The one-dimensional heat conduction assumption only accounts for the transverse heat flux trough the wall between two fluids. It does not account for 2D longitudinal heat conduction in the tube and it neglects the longitudinal heat conduction in the fin, along the air flow direction. Asinari et al. (2004) concluded that these effects produce a negligible effect on the performance of the class of CO_2 gas cooler they studied.

A gas cooler working with CO_2 in supercritical pressures is an application where a large impact on the performance could be expected due to 2D LHC in the tube wall and heat conduction between tubes trough fins. The reasons are based on the temperature glide of CO_2 during a supercritical gas cooling in contrast with a condenser where the temperature during condensation is approximately constant. Representative values can be extracted from experimental results of Zhao et al. (2001) where CO2 undergoes temperature variations along a single tube from 25 K up to 85 K while maximum temperature difference between two neighbour tubes range from 30 K to 100 K.

This paper presents a detailed model for microchannel heat exchangers used as gas coolers which does not use the fin efficiency, accounts for 2D LHC in fins and tubes, accounts for the heat conduction between tubes, and applies a detailed discretizastion for the air, which is independent of the refrigerant discretization. The model, referred to as Fin2D, subdivides the heat exchanger into segments and cells (air, refrigerant, fin, tube wall), to which a system of energy conservation equations is applied without traditional heat exchanger modelling assumptions. Fin2D differs from other models referred to previously in the number of classical assumptions made. The model of Asinari et al. (2004) is the most similar to the present model regarding the number of assumptions, although the discretization method applied by them is a hybrid one, which uses both the finite-element method (FEM) and the finite volume method (FVM), whereas the methodology used in the Fin2D model is the FVM.

After a numerical verification, the solution obtained with the Fin2D model is employed to assess the impact of the classical heat exchanger modelling assumptions on the accuracy of the performance predictions for such conditions. The goal of the present work is to study the heat transfer processes in a microchannel gas cooler by evaluation of each of individual heat transfer effects described above, rather than propose a model able for heat exchangers design. The present work will also provide a deeper understanding of the microchannel CO_2 gas coolers.

2. Fin2d heat exchanger model

2.1. *Heat exchanger discretization*

Fig. 1(a) presents a piece of the studied microchannel heat exchanger. It is discretized along the X direction (refrigerant flow) in a number of segments *a*. Each segment (Fig. 1(b)) consists of: two streams of refrigerant (top and bottom flows)

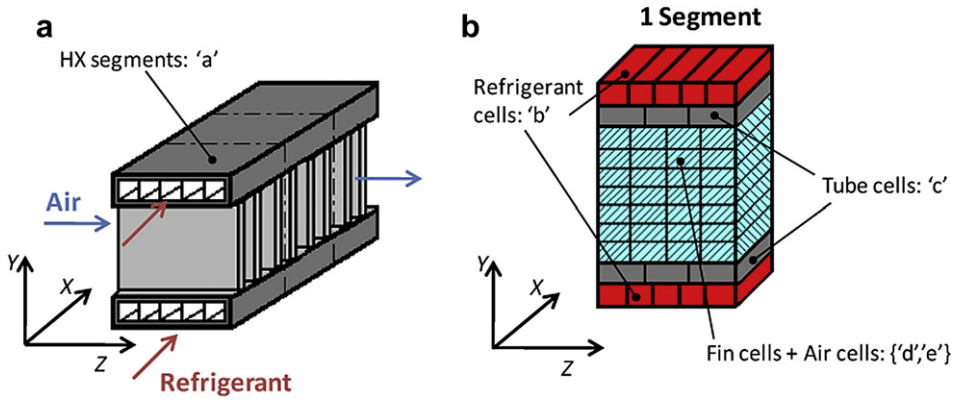

Fig. 1 – (a) Piece of the heat exchanger studied in the paper. (b) Schematic of the discretization applied in a segment of the heat exchanger.

that are split into b channels in the Z direction (air flow); two flat tubes (top and bottom) that are discretized into c cells in the Z direction; and both air flow and fins, which are discretized in two dimensions: d cells in the Y direction and e cells in the Z direction. This discretization is summarized in the text as; grid: {a,b,c,d,e}. For illustration of the nomenclature, the numerical example shown in Fig. 1(a) and (b) corresponds to a grid: {3,5,3,7,4}.

The refrigerant flows inside the channels ($b = 5$ in Fig. 1(a)) along the X direction without any mixing between the channels, and it exchanges heat with the tube cells in contact; these tube cells transfer this heat to the air cells in contact by convection, and to its neighbouring tube cells on the plane X-Z and to the fin roots in contact by conduction. The air exchanges heat by convection with the fin cells, and the air cells at the bottom and top also exchange heat with the tube cells in contact. The fin cells conduct the heat along the plane Y-Z, and the bottom and top fin cells also conduct heat to the tube wall.

2.2. Governing equations

Every fluid cell (refrigerant or air) has two nodes, which correspond to the inlet and the outlet in the fluid flow direction. The wall cells (tube or fin) have only one node located in the centroid of the cell, as is shown in Fig. 2(a). All cell's local variables are referred to the value in these nodes, e.g. $T_{i,in}$ and $T_{i,o}$ are the temperature at the inlet and at the outlet, respectively, of a fluid cell i, either refrigerant or air. T_{wj} is the temperature defined for the wall cell j, which could be either fin or tube.

In this situation the governing equations at each fluid cell (refrigerant and air) and at each wall cell (tube and fin) can be written as follows:

$$\dot{m}_i \, dh_i = \sum_{j=1}^{n_i} \dot{q}_{ji} \, P_{ji} \, ds_i \tag{1}$$

$$\dot{q}_{ji} = U_{ji} \left(T_{wj} - T_i \right) \tag{2}$$

$$U_{ji} = \frac{1/A_{ji}}{\dfrac{t_j/2}{A_{ji}\, k_{j,k}} + \dfrac{1}{A_{ji}\, \alpha_{ji}}}$$

$$\nabla \left(k_{j,k} \, t_j \, \nabla T_{wj} \right) + \sum_{i=1}^{n_j} \dot{q}_{ji} = 0 \tag{3}$$

where any wall cell j is in contact with n_j fluid cells $i = 1, n_j$; any fluid cell i is in contact with n_i wall cells $j = 1, n_i$; $k_{j,k}$ is the thermal conductivity of the wall cell j in the k direction, thus it is possible to study the influence of 2D LHC at both fin and tube walls. Eq. (1) states the energy conservation for a fluid cell, whereas Eq. (3) states the energy conservation for a wall cell. Eq. (2) represents the heat flow between a wall cell and a fluid cell. Neither pressure losses nor dehumidification has been modelled since it is a gas cooler and the paper only focuses on the understanding of possible differences in heat transfer.

For solving the system of equations a set of boundary conditions is needed. Inlet conditions and velocity distributions are known for both fluids, and velocity distribution is assumed as uniform. Since the heat exchangers are normally well insulated, the heat transferred by the wall edges to the surrounding is considered negligible, and the wall cells are considered to be adiabatic with the surrounding. Only two tubes of the whole gas cooler are going to be modelled in this work, so an additional boundary condition is necessary: both tubes have symmetry condition. This symmetry condition implies that the heat transferred from a tube to each of the neighbouring tubes is the same. This assumption approximates simulations at central tubes of a microchannel slab. It has to be noted that this symmetry condition does not mean that the heat transferred by each tube have to be the same, in fact it will be studied in Section 6.

For the discretization of equations the finite volume method (FVM) (Patankar, 1980) has been applied along with the semi-explicit method for wall temperature linked equations (SEWTLE) proposed by Corberán et al. (2001). The discretization of governing equations does not present any special difficulty, except for the estimation of the integral of

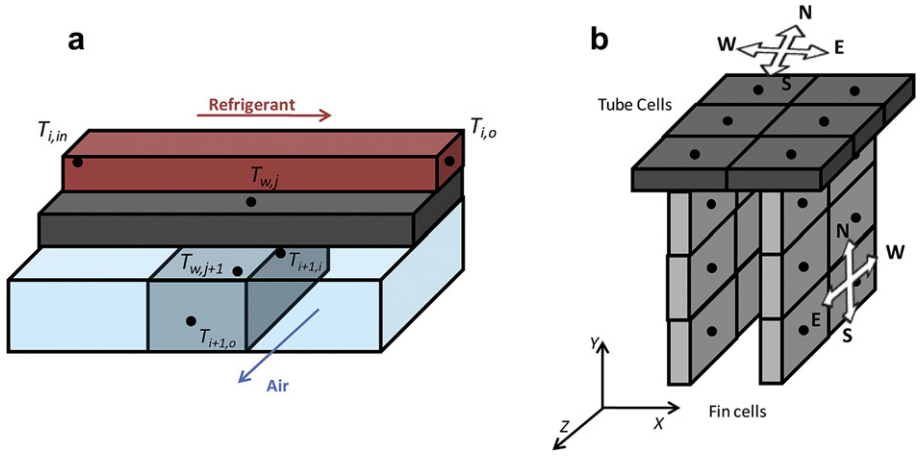

Fig. 2 – (a) Cells schematic and definition of the cell nodes. (b) Direction references for fin and tube wall cells.

the heat transferred to the fluids in contact with a considered piece of wall (Eq. (2) and (3)). This integration must be consistent with the integration of the coincident terms of fluid energy Eq. (1). The numerical scheme corresponding to a linear fluid temperature variation (LFTV), as explained in Corberán et al. (2001), is employed for the discretization of Eq. (2). This numerical scheme is basically based on assuming a piecewise distribution of the fluid temperature along the fluid cell, leading to the following expression:

$$A_{ji}\,\dot{q}_{ji} = U_{ji}P_{ji}\left(T_{wj} - \frac{T_{i,in}+T_{i,out}}{2}\right)\Delta s_i \tag{4}$$

The discretization of the Laplacian operator in Eq. (3) has been made by the classical finite difference approach according to the adopted FVM. The Eq. (3) discretization used in this model is shown in Eq. (5).

$$a_j\,T_{wj} - \sum_{k=W,E,S,N} a_{j,k}\,T_{wj,k} = a_{j,J}\,T_{wj,J} - \sum_{i=0}^{n_j} P_{ji}\,U_{ji}\,(T_{wj}-T_i)\,ds_{ji} \tag{5}$$

$$a_{j,W} = \frac{k_{j,W}\,Ac_{j,W}}{\delta l_{j,W}} \quad a_{j,E} = \frac{k_{j,E}\,Ac_{j,E}}{\delta l_{j,E}} \quad a_{j,S} = \frac{k_{j,S}\,Ac_{j,S}}{\delta l_{j,S}}$$
$$a_{j,N} = \frac{k_{j,N}\,Ac_{j,N}}{\delta l_{j,N}} \quad a_{j,J} = \frac{k_{j,J}\,Ac_{j,J}}{\delta l_{j,J}} \quad a_j = \sum_{k=W,E,S,N,J} a_{j,k}$$

All $a_{j,k}$ terms refer to the conductance between a wall cell j and the neighbouring wall cell, adjoined to this one, in the direction k. The direction reference is different in the tube and fin cells; the schematic used in the model is shown in Fig. 2(b). There is one exception: $a_{j,J}$, which means the conductance of the joint between a tube wall cell and a fin wall cell.

The global solution method is outlined in Corberán et al. (2001). Basically, this method is based on an iterative solution procedure. First, a guess is made about the wall temperature distribution, and then the governing equations for the fluid flows are solved in an explicit manner, getting the outlet conditions at any fluid cell from the values at the inlet of the heat exchanger and the assumed values of the wall temperature field. Once the solution of the fluid properties is obtained for any fluid cell, then the wall temperature at every wall cell is estimated from the balance of the heat transferred across it (Eq.(3)). This procedure is repeated until convergence is reached. The numerical method employed for calculating the temperature at every wall cell is based on the line-by-line strategy (Patankar, 1980) following the Y direction for fin cells and the X direction for tube cells, so that the global strategy consists of an iterative series of explicit calculation steps. This method can be applied to any flow arrangement and geometrical configuration, and offers excellent computational speed. Additionally, it can easily be extended to other cases, such as two-phase flow or humid air.

3. Case study

In this case study we modelled a microchannel gas cooler for which dimensions were extracted from Zhao et al. (2001). Since the objective of this work was to evaluate the effects of different classical assumptions in the predicted results, operating conditions that produce large temperature variations and high heat fluxes were of interest. Consequently, the chosen operating conditions correspond to the experimental data of the test for gas cooling n 3b, HX1, from the same work. Table 1 shows the most important geometric data while Table 2 shows the considered operating conditions. Some data were estimated from the reported experimental values; namely, the CO_2 side heat transfer coefficient was estimated to be 537 W m^{-2} K^{-1}. This coefficient was estimated by using the ε-NTU relationship for cross-flow (Incropera and DeWitt, 1996) working in the mentioned test conditions. For these calculation the air-side heat transfer coefficient was required and it was evaluated with convection correlation for fully laminar flow in non-circular tubes (Incropera and DeWitt, 1996) resulting to be 66 W m^{-2} K^{-1} (this value will be used only in the verification studies).

Table 1 – Geometry of the microchannel heat exchanger.

Tube length (cm)	8	Fin pitch (mm)	1.56	Channel diameter (mm)	1
Tube depth (mm)	16	Fin thickness (mm)	0.152	Channels number	10
Tube thickness (mm)	1	Fin height (mm)	8		

The heat transfer mechanisms that take place along a tube in a gas cooler depend neither on the tube length nor the number of tubes. For this reason, only an equivalent piece of the heat exchanger has been considered in the detailed analysis of the heat transfer.

The reference case study is shown in Fig. 3(a). It consists of two central tubes with their fins attached. The total length of the tubes is five times the tube depth. The refrigerant has only one pass along the heat exchanger with the same mass flow rate in both tubes.

For the evaluation of the thermodynamic and transport properties of fluids, REFPROP (Lemmon et al., 2002) was used. The air, properties were locally evaluated whereas the refrigerant properties were assumed as uniform and evaluated as averaged values between the corresponding values at the inlet and the outlet of the heat exchanger studied in the present work. The thermal conductivity of the fin and tube walls was estimated to be 173 W m^{-1} K^{-1}.

4. Numerical verification of the Fin2d model

Before employing the newly developed model to produce detailed solutions of heat transfer in the equivalent piece of the microchannel gas cooler, shown in Fig. 3(a), it is necessary

Table 2 – Operating conditions; Test for gas cooling n 3b, HX1 (Zhao et al., 2001).

	Inlet pressure (kPa)	Inlet temperature (°C)	Outlet temperature (°C)	G (kg/m^2 s)
CO_2	8937	79.9	42.4[a]	132.56
Air	100	23.74[a]	32.4	3.05

a estimated value.

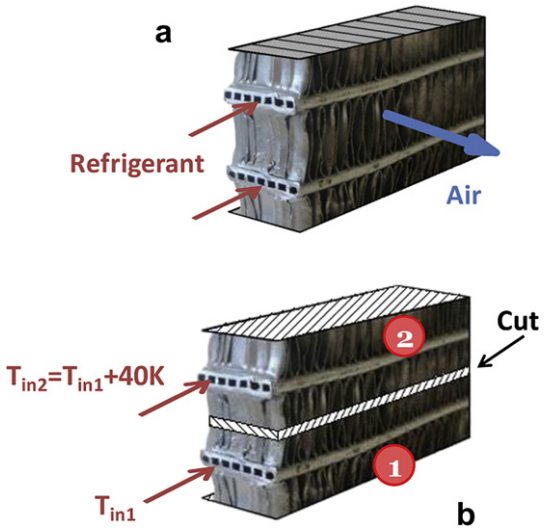

Fig. 3 – (a) Schematic of the equivalent heat exchanger studied. (b) Schematic of the equivalent heat exchanger used in the study of the adiabatic-fin-tip assumption.

to validate the model. With this purpose in mind we performed a series of systematic checks against operational cases for which an analytical solution can be obtained.

The detailed discretization of the air flow in the Y direction adopted in Fin2D makes it difficult to compare Fin2D predictions with those of analytical solutions. In order to validate the model, many scenarios, listed below, were simulated. These scenarios have an analytical solution, and this solution was adopted as a reference to evaluate the error of the Fin2D model. The following, are different studied scenarios:

- Air-side verification (V1): For the refrigerant, the infinite heat capacity rate ($\dot{m}\cdot C_p$) was imposed, which means no temperature change for the refrigerant. Also, we disabled the 2D LHC in the tube walls (LHC_x and LHC_Z) and the LHC_Z in the fin, since these effects are not accounted for by the available analytical solutions. The detailed discretization of the air volume, in the Fin2D model, accounts for a non-uniform air temperature along the Y direction. Since this effect is not taken into account by any analytical solution, the fin and air were only discretized in the X and Z directions, using only one cell along the Y direction, to make a valid comparison of the Fin2D model with analytical solution. On the other hand, it is not possible to capture the fin temperature variation with only one fin cell along the Y direction. Thus, the value of the thermal conductivity for the fin in this direction was set as infinite. In this situation the fin efficiency was equal to 1, and the fin wall temperature was uniform along the Y direction. Finally, constant properties and heat transfer coefficients were used, which correspond to those exposed in Section 3. For this scenario the analytical solution for the heat exchanger effectiveness is $\varepsilon = 1\text{-}\exp(\text{-NTU})$.
- Refrigerant side verification (V2): The methodology applied was the same as for V1, but the fluid with infinite heat capacity rate was the air. Now, the results were not as sensitive to the air discretization as it was in the V1 case because the air has infinite heat capacity rate and its temperature change is negligible.
- Fin temperature profile verification (V3): The fin conductivity in the Y direction had a value corresponding to the case study. Two cases were studied: with the same and different fin root temperatures. The analytical solutions for both cases were taken from Incropera and DeWitt (1996). These relationships assume a uniform air temperature along the Y direction, and uniform air properties and heat transfer coefficient. Thus, to avoid the air temperature change along the Y direction, the infinite air flow-stream heat capacity rate ($\dot{m}\cdot C_p$) was imposed. The refrigerant flow-stream capacity rate was also assumed to be infinite to obtain a uniform tube wall temperature along all fin roots. The fin was discretized only in one cell along the Z direction so there was no LHC_Z in the fin.
- Two-dimensional heat conduction in the wall (V4): This case validates the discretization of the Laplacian term of Eq. (3). This case studies 2D LHC in the tube assuming no convection and no thermal joint between the fin and the tube. A set of temperatures for each wall's edge was imposed. The analytical solution for this situation can be obtained solving the Laplacian equation for a flat plate given temperatures at the edges.

Fig. 4 shows the error of the numerical solution with reference to the analytical solution for V1 and V2 cases. The error tends to diminish very quickly with the number of cells used (N). In the case of V1, the abscissa shows the number of cells in the Z direction. As it can be observed, the error is very small already for $N = 5$. In the case of V2, where the air has the infinite flow-stream capacity rate, the abscissa was taken as the number of cells along the X direction. Again the analytical solution is almost reached with only five cells.

Regarding the case V3 verification, Fig. 5 shows the error of the numerical solution for the heat transferred from the air film to the fin wall as a function of the number of cells in the Y direction for two situations: equal temperatures of the bottom tube and the top tube, and a temperature difference between

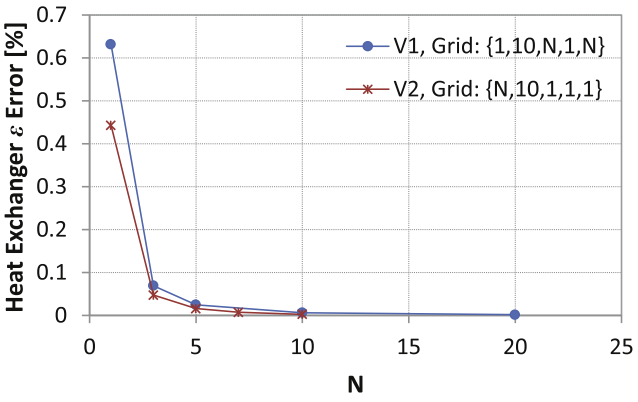

Fig. 4 – Validation results for two scenarios: air-side when the number of cells in the Z direction is varied (V1), and refrigerant side when the number of segments in the X direction is changed (V2).

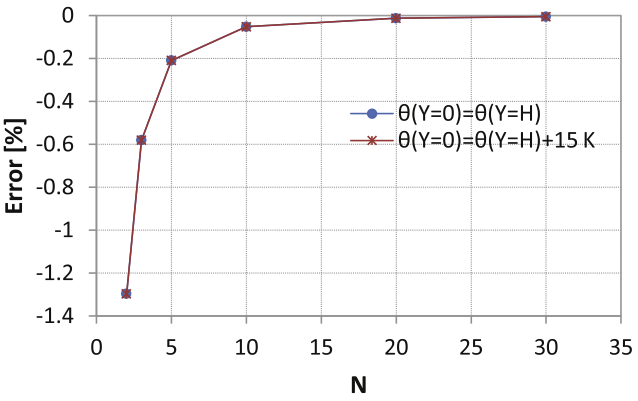

Fig. 5 – Fin temperature profile validation (V3): Error of the heat transferred from the fin to the air, for two cases: tubes with the same temperature and with a temperature difference of 15 K, with the grid: {1,1,1, N,1}.

tubes of 15 K. θ is a difference between the fin temperature and the air temperature. As can be observed, the error is small, −0.2%, with only five cells in the Y direction, and quickly approaches zero. The calculated fin temperature profile is shown in Fig. 6(a) and (b) for the V3 study in the same two previous cases. The grids differ by the number of fin cells in the Y direction. In this manner the accuracy of the numerical model is proved.

Finally, in order to validate the 2D LHC in the Fin2D model, Fig. 7(a) presents results for case V4, where the boundary conditions were: T(X/L = 0) = 70 °C, T(X/L = 1) = 50 °C, T(Z/D = 0) = 25 °C, T(X = 0) = 35 °C. Fig. 7 (b) shows the error in the wall temperature field evaluated as a deviation of the Fin2D results from the theoretical solution. It is noticeable that the error ranges from −0.1 K and +0.1 K over almost the entire plate, which is considered as acceptable. The error increases up to 1.3 K only locally near the corners. The reason is that the actual temperature field imposed along the tube edge is discontinuous just at the corners. The Fin2D model can obtain only continuous solutions, so near the corner the error is increased. This study was also carried out for the fin, resulting in similar results.

5. Case study solution

In this section the Fin2D model is used to solve the case study problem. Many thermal variables are analyzed in order to understand the actual heat transfer mechanisms in the case study using a very detailed model able to capture fin and tube two-dimensional temperature profiles, the refrigerant temperature profile in each channel, and the air temperature profile along the direction between tubes.

This study used test conditions presented in Table 2. The air-side heat transfer coefficient was estimated by correlations for a plain fin following the recommendations of Webb (1994). The heat transfer coefficient obtained with this correlation is referred to as α_{air}. Two scenarios were considered: with the air-side heat transfer coefficient equal to α_{air}, and with a value three times larger, consequently the air-side heat transfer coefficient ranged from 60 W m^{-2} K^{-1} to 180 W m^{-2} K^{-1}. This choice was made to cover large variations of possible fin surfaces including enhanced fin surfaces with a high heat transfer coefficient.

Regarding the refrigerant side, constant properties and heat transfer coefficients were used, as listed in Section 3. Since the tube length was short, the refrigerant property variations are expected to be negligible; the refrigerant is a gas far from the critical point at which properties change drastically.

In order to set a grid size to obtain the solution in each scenario, with the required accuracy for the comparisons done in this work, the authors studied the results accuracy when the grid dimensions were changed. From a very detailed grid, the different grid dimensions were reduced until a further refinement of the grid did not lead to a significant increase in accuracy. The adopted grid dimensions were: {3,10,10,30,10}, following the nomenclature explained in Section 2.1. The capacities obtained for this case study were 24.21 W and 33.6 W for the scenarios with $\alpha_{air} = \alpha_{air}$ and $\alpha_{air} = 3\ \alpha_{air}$, respectively.

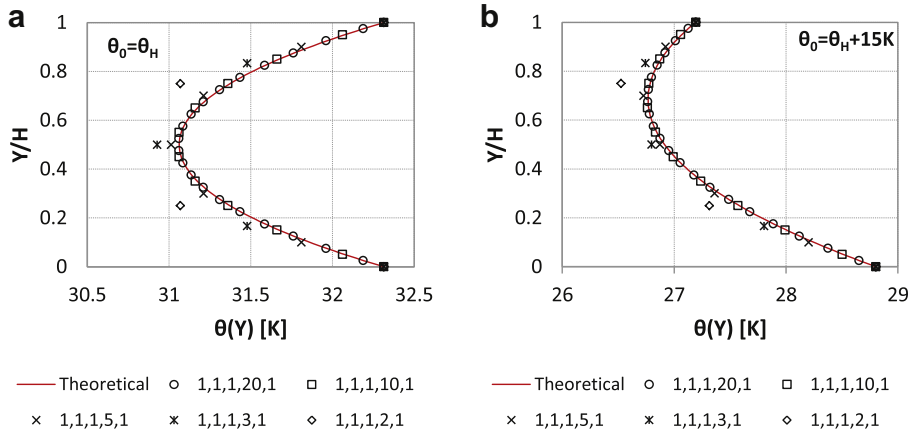

Fig. 6 – Fin temperature profile validation (V3): (a) the case with the same inlet tube temperatures and (b) the case with a temperature difference between tubes of 15 K (five grids considered).

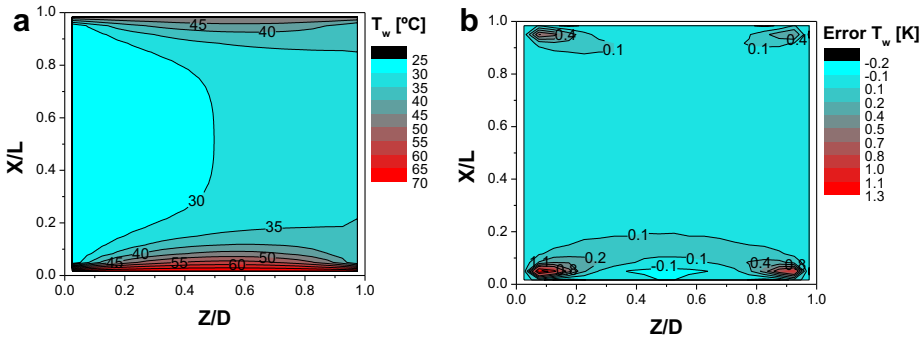

Fig. 7 – Two-dimensional conduction (V4): (a) Tube temperature profile predicted with the Fin2D model. (b) Error, evaluated as temperature difference, of the Fin2D model with respect the analytical solution.

First, results for the refrigerant are shown in Fig. 8(a) and (b). Fig. 8(a) presents the refrigerant temperature evolution along the X direction. Fig. 8 (b) presents the temperature profile as a function of the dimensionless tube depth (Z direction) at $X = 0.833$. In this figure, a case with one equivalent channel (same hydraulic diameter and cross area) is also plotted in order to study the differences between modelling the actual number of channels and modelling all the fluid as an equivalent fluid cell with the assumption of mixed refrigerant along the tube.

In Fig. 8 (b) the temperature profile for 10 channels describes a typical trend when 2D LHC in the tube is present. It is noticeable how small the temperature variation between different refrigerant channels is in both scenarios (at most 0.5 K). The difference in the total capacity calculated resulted to be less than 0.005% for both scenarios. This is due to two reasons: the uniform refrigerant temperature for the one channel case almost coincides with the averaged value of the refrigerant temperature in the multichannel case, and the uniformity of the tube temperature along the Z direction. The combination of these two facts produces an equal averaged difference of temperatures between the tube and the refrigerant, which produces the same capacity transferred by the fluid. Thus, for the scenario studied, the modelling of a minichannel tube as one equivalent channel introduces a negligible error.

To analyze the thermal evolution of the air, Fig. 9 presents air temperature profiles along the Y direction at the refrigerant inlet ($X = 0$) at three different locations along the Z direction. The detailed air discretization makes it possible to study the variation of the air temperature not only along its flow rate direction but also in the direction between tubes. In Fig. 9, we can observe that the temperature of most of the air is uniform, except the air close to the tube wall. Only for a high value of the air-side heat transfer coefficient (about 180 $W\,m^{-2}\,K^{-1}$) the air undergoes a small temperature variation along the Y direction. This observation agrees quite well with the assumption used in the fin theory development. But, the temperature of air close to the tube wall is higher by up to 15 K with respect to the rest of the air, and this fact is not taken into account in the fin theory development.

Finally, similarly to the aim of Fig. 9 to study the air flow evolution, Fig. 10 (a) and (b) were plotted to study the fin temperature field at the refrigerant inlet section ($X = 0$). When $\alpha = \alpha_{air}$ the temperature field is quite similar to that for a one-dimensional field since the temperature gradient is almost negligible along the Z direction. However, when the air-side heat transfer coefficient increases, due to the fact that the air temperature variation along the Z direction significantly increases, a strong temperature gradient in the Z direction appears along the fin, leading to a considerable effect of the

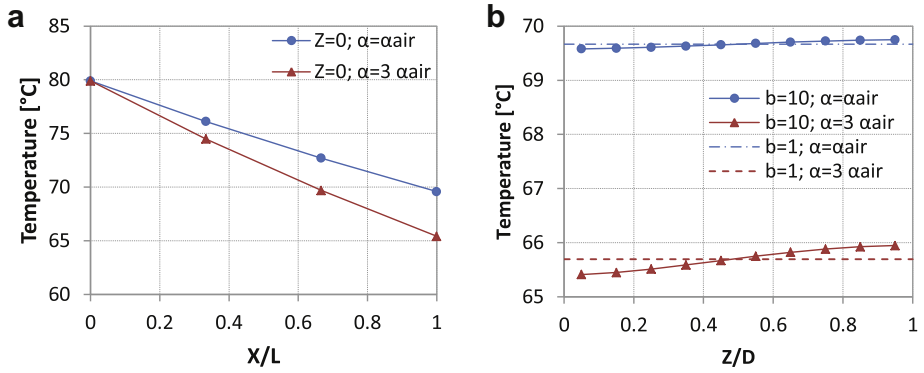

Fig. 8 – (a) Refrigerant temperature evolution along the tube length for two values of the air-side heat transfer coefficient. (b) Refrigerant temperature profile along the Z direction for two values of the air-side heat transfer coefficient. Each scenario was studied using the actual number of channels ($b = 10$) and one equivalent channel ($b = 1$).

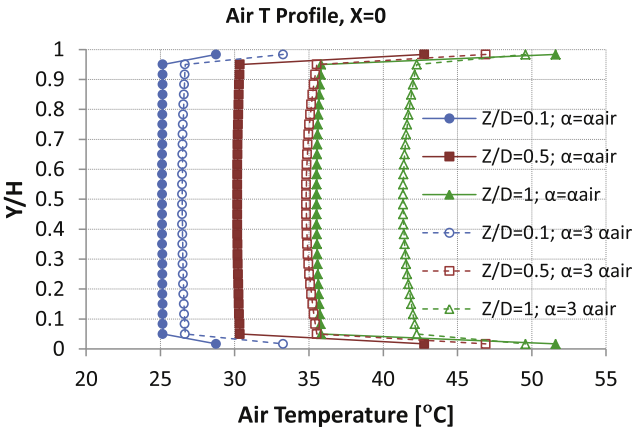

Fig. 9 – Air temperature profiles along the Y direction at the refrigerant inlet (X = 0) for three locations along the Z direction.

LHC_z. This fact points out the big impact of the air-side heat transfer coefficient on these profiles.

Fig. 11 (a) and (b) present the temperature fields for the tube wall. Again, the results depend strongly on the air-side heat transfer coefficient. When the air-side heat transfer is low, basically only the LHC_x in the tube is present, but when this coefficient increases the effects of LHC_Z in the tube also become visible since there is a temperature gradient on the wall tube along the Z direction.

The impact of 2D LHC in the tube and LHC_Z in the fin on the solution are discussed in the following section.

6. Analysis of the segment-by-segment ε-NTU modelling and effect of classical assumptions

Once the Fin2D model has been validated it can be used as a reference to check the relative error made by the segment-by-segment ε-NTU modelling of a gas cooler and for studying the impact of the classical assumptions, which are implicit in this methodology. In order to evaluate the relative error, the reference used in this evaluation was the solution for the case study at the same operating conditions and applying the same grid size.

The classical ε-NTU modelling approach divides each heat exchanger tube into segments along the refrigerant flow with its corresponding fins. Some authors use only one segment per tube, which is commonly referred to as the tube-by-tube approach. When the tube is discretized in more than one segment (N) the approach is defined as the segment-by-segment approach. Once the heat exchanger is divided into segments, the ε-NTU relationships for heat exchangers (Incropera and DeWitt, 1996) are employed for each segment. For multichannel cross-flow heat exchangers the air is always considered to be unmixed because the fins prevent the mixing, but there are two options for the refrigerant: to assume the refrigerant as mixed (RMAU) or as unmixed (BU). In a multichannel tube, the refrigerant is actually unmixed, but some authors assume the refrigerant flow as mixed, applying the RMAU relationship in a segment-by-segment approach, e.g. Jiang (2003). However some other authors, e.g. Fronk and Garimella (2011), apply the BU relationship using also a segment-by-segment approach. Thus, there is no full agreement in the literature regarding using the RMAU and BU options.

The ε-NTU models used in this analysis were developed within Engineering Equation Solver (Klein, 2004). Both options available within the ε-NTU modelling methodology were included in this study: BU and RMAU. The ε-NTU models used the same properties and heat transfer correlations as those used in the Fin2D model.

The classical ε-NTU modelling presents the following drawbacks:

- 2D LHC: As it was explained in the introduction, the ε-NTU method does not account for 2D LHC in the tube (LHC_x and LHC_Z) and LHC_Z in the fin.
- Adiabatic-fin-tip efficiency: This assumption is widely used even when a temperature difference between tubes exists.
- Discretization inconsistency of the BU option: discretizing along the X direction, i.e. introducing number of segments (N), involves an implicit mixing of the refrigerant stream since the inlet temperature at one segment is evaluated as the averaged value at the outlet section of the preceding segment. Consequently, for the BU ε-NTU case, increasing the number of segments is inconsistent with the hypothesis of unmixed refrigerant stream. Therefore, if the unmixed condition for the refrigerant is the one which better represents the actual process, the best option for the

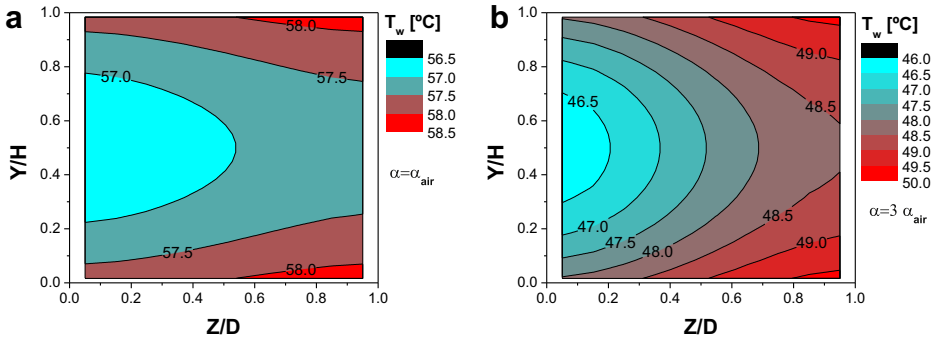

Fig. 10 – Fin wall temperature profile at the refrigerant inlet section (X = 0) for the case study with: (a) $\alpha = \alpha_{air}$ (b) $\alpha = 3\ \alpha_{air}$.

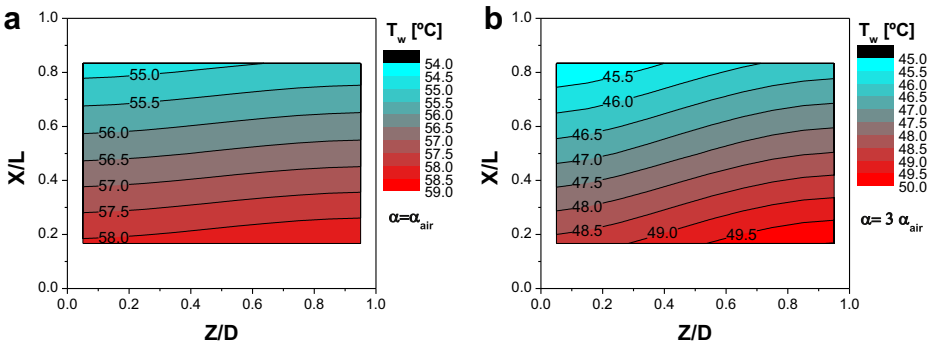

Fig. 11 – Tube wall temperature profile for the case study with: (a) $\alpha = \alpha_{air}$ (b) $\alpha = 3\ \alpha_{air}$.

discretization along the X direction would be to employ a tube-by-tube approach. This will lead to a full consistent BU solution at each tube with mixing at the outlet. This mixing would be perfectly consistent with the real operation in those microchannel heat exchangers where the tubes end in the collector/distributor head. For serpentine heat exchangers, the BU solution is not consistent because the refrigerant is mixed.

- Air temperature variation along the Y direction: the ε-NTU approach assumes that the air temperature is constant along the Y direction since the ε-NTU approach uses the fin theory, which is developed under this assumption. This assumption deviates from the reality because the temperature of the air flowing close to the tube and the fin roots becomes much closer to the wall temperature, as it was shown earlier.

It is important to notice that most of the models for heat exchangers are based on the classical assumptions analyzed above. Therefore, although they do not employ ε-NTU approach, they suffer of some of the drawbacks commented above, except the BU discretization inconsistency, that is exclusive for ε-NTU models.

6.1. *Comparison of Fin2D model against ε-NTU approaches*

The scenarios used to analyze differences between simulation predictions by the Fin2D model and the classical ε-NTU approaches are the same as those used for the case study solution. In gas coolers such as serpentine or multitube heat exchangers with large number of refrigerant passes, large temperature differences can appear between the refrigerant in neighbouring tubes. In order to study the heat transfer in these gas coolers, a new scenario has been added to the simulation studies. This scenario modifies the cases presented previously by introducing a temperature difference between refrigerant inlets of 40 K, as shown in Fig. 3(b).

Fig. 12 (a) and (b) quantify the relative errors obtained when using the classical ε-NTU approaches. In these figures N represents the number of segments used to discretize the tube length. For the RMAU case, the trend of the ε-NTU model is asymptotic to the Fin2D solution with a final error of 2.5% for the α_{air} case, which increases to 3.5% for the air-side heat transfer coefficient value increased threefold (to about 180 W m^{-2} K^{-1}). The simulations carried out for the scenario with different refrigerant inlet temperatures resulted in identical results, which means that the error does not depend on a temperature difference between the tubes.

For the BU case, the errors are smaller, below 1.5%, indicating that this approach is much closer to the Fin2D solution. However, as it can be observed in Fig. 12 (b), the error increases with the increasing number of cells. This problem is a result of the modelling inconsistency that was pointed out and explained above. Following that explanation, it would be consistent with the assumption of unmixed refrigerant made for the BU case to use only one cell per tube; however, Fig. 12(b) shows the most accurate solution when $N = 2$. The reason for

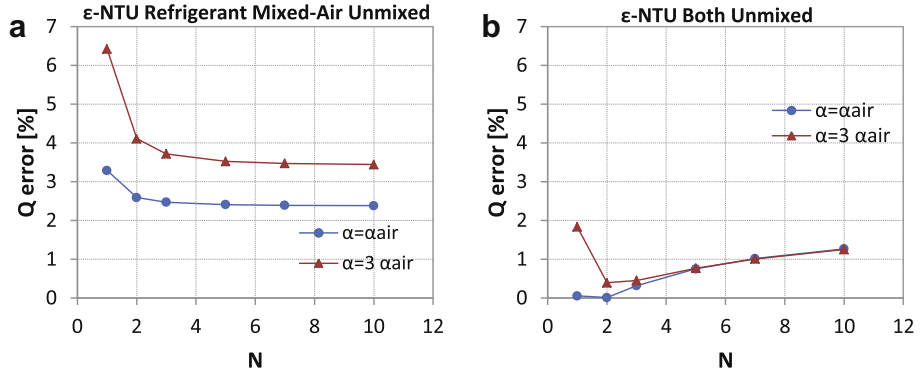

Fig. 12 – Comparison of Fin2D model and ε-NTU model for different number of refrigerant segments (N) in the X direction used by the ε-NTU model: (a) using RMAU relationships, (b) using BU relationships.

this result and trend is not clear since many effects occur simultaneously. The main reason could be that one segment ($N = 1$) produces a linear temperature distribution for the fluids and a poor discretization of the problem, thus when the number of segments is increased, the accuracy is improved despite the modelling inconsistency. But with values N larger than two segments, the modelling inconsistency takes an overriding influence on the accuracy, and the error begins to increase.

After observing these results it could be thought that the effect of the temperature difference of the refrigerant between neighbouring channels is important. However, Fig. 8 (b) and the comments made regarding Fig. 8(b) in the previous sections do not support this idea.

6.2. Analysis of classical assumptions with Fin2D model

This section analyzes the impact of individual classical assumptions used in a heat exchanger model on the simulation results. The impact was evaluated with respect to the complete Fin2D model prediction by imposing selected assumptions within the Fin2D model, and performing additional simulations. The considered assumptions are: no 2D LHC in the tube, no LHC_Z in the fin, adiabatic-fin-tip, and uniform air temperature along the fin height (Y direction). The case study CO_2 gas cooler was used in these simulations.

6.2.1. LHC effects

To evaluate the impact of the LHC effects and to identify the most dominant areas with heat flow and its direction, four cases of simulations were performed with the following modelling constraints: (1) no LHC_Z in the fin, (2) no LHC_x in the tubes, (3) no LHC_Z in the tubes, and (4) all LHC effects disabled for all wall elements, except conduction along the Y direction in the fin. Table 3 shows the error in the capacity predictions associated with eliminating from consideration selected LHC phenomena with respect to the complete solution (case study solution which includes LHC in all elements and directions enabled) and same refrigerant inlet temperature.

The effect of LHC depends strongly on the air-side heat transfer coefficient. When the air-side heat transfer coefficient is equal to the reference value, α_{air}, the influence of LHC is negligible. But when the air-side heat transfer coefficient has a three times as high value (about 180 W m^{-2} K^{-1}), the effect is noticeable, 2.54%. This impact increase, when the air-side heat transfer is increased, can be explained by observing Figs. 10(b) and 11(b). In these figures the temperature gradient along the Z direction in the fin and along the X and Z directions in the tube rises when the air-side heat transfer coefficient increases, whereas the temperature gradient along the Z direction in the tube and fin is almost negligible for the lowest air-side heat transfer coefficient value.

This increase in the prediction error due to neglecting the LHC effects when the air-side heat transfer coefficient is increased is consistent with the increase in the prediction error shown in Fig. 12(a) for the ε-NTU models. When the LHC has the largest influence, the dominant component is the LHC_Z in the tube. It is important to notice that the LHC effects are strongly non-linear.

The case with a temperature difference between tubes was also studied in the same way as described above. The results and conclusions are the same. This fact indicates that the LHC effects in an element do not depend on the conditions of its neighbouring elements. These conclusions are not valid for the heat conduction in the fin between tubes, which is studied below.

Table 3 – Effect of 2D LHC on capacity.

	Q error case 1 [%]	Q error case 2 [%]	Q error case 3 [%]	Q error case 4 [%]
$\alpha = \alpha_{air}$	0.03	0.12	0.09	0.66
$\alpha = 3\ \alpha_{air}$	0.24	0.10	0.55	2.54

6.2.2. Adiabatic-fin tip

To study the effect of assuming the adiabatic tip at the half length of the fin, as it is usually accepted, the case with the 40 K temperature difference between refrigerant inlets was chosen, since the adiabatic-fin-tip assumption is exact for the case with the same refrigerant inlet temperature. To quantify this error and isolate only the effect of the adiabatic-fin-tip assumption, this scenario was modelled by introducing a cut along the fin surface and leaving all remaining LHC effects enabled. The cut was modelled as a cut along the air direction in the middle section of the fin surface between tubes (Fig. 3(b)). Under these conditions the adiabatic-fin-tip assumption is strictly correct, even though there is a temperature difference between neighbouring tubes. Thus, the difference between results for a scenario solved with and without modelling a cut along the fin corresponds to assuming an adiabatic-fin-tip when a temperature difference between tubes exists.

Table 4 contains a summary of the obtained results. Tubes 1 and 2 referred to in this table are depicted in Fig. 3(b). The difference between the capacity with the fin cut and without it is negligible, which means that the improvement in the capacity is almost zero. Nevertheless, Table 4 shows large errors, more than 300%, in the heat capacity per tube calculated assuming adiabatic-fin-tip efficiency with respect to using the actual fin efficiency. These deviations produce a different heat flux distribution in the gas cooler. In fact, these result agrees with the findings of Asinari et al. (2004) who explained that the total heat transferred by the fin between two tubes (sum of the heat flux for both fin roots) is exactly the same assuming either the adiabatic-fin-tip or the actual one, independently of the temperature difference between neighbouring tubes. They studied a three passes gas cooler, and concluded that the impact of adiabatic-fin-tip assumption involves a modest effect on the total capacity prediction, about 1%. However, Park and Hrnjak (2007) reported improvements in capacity up to 3.9% by cutting fins for a microchannel serpentine gas cooler. A possible explanation of this contradiction is that the effect, of the heat flux distribution in the gas cooler on the total heat capacity, depends of the number of passes. It results in a noticeable total capacity difference when the number of passes is large, as is the case of the serpentine

Table 4 – Effect of assuming adiabatic-fin-tip efficiency on capacity.

	Q without fin cut [W]	Q with fin cut [W]	Q without fin cut tube 1 [W]	Q error tube 1 [%]	Q without fin cut tube 2 [W]	Q error tube 2 [%]
$\alpha = \alpha_{air}$	15.35	15.37	−1.87	−274.87	17.22	−29.73
$\alpha = 3\ \alpha_{air}$	21.32	21.35	1.1	313.64	20.23	−16.96

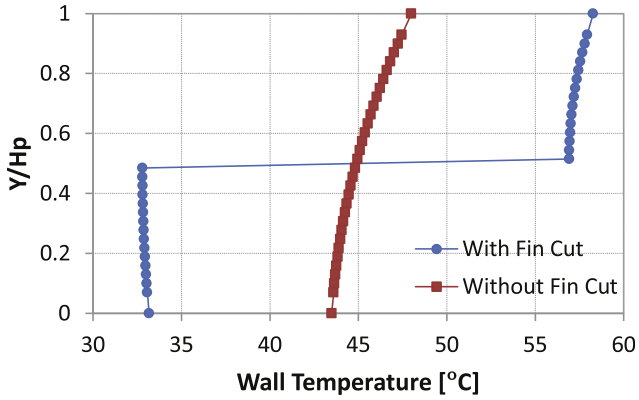

Fig. 13 – Wall temperature profile (fin and tubes) along the Y direction at the refrigerant inlet section (X = 0) in the middle of the tube depth (Z/D = 0.5) for both scenarios solved with Fin2D model: fin cut and without cut, $\alpha = \alpha_{air}$.

gas cooler studied by Park and Hrnjak (2007). Currently, Fin2D does not have the capability to simulate complex circuitry arrangement to validate the above hypothesis, but the work to enhance Fin2D in this direction is underway.

The wall temperature profiles for each solution (when $\alpha = \alpha_{air}$) are plotted in Fig. 13. The profiles are shown along the Y direction at the refrigerant inlet section ($X = 0$) in the middle of the tube depth. The error in the capacity of the fin roots, explained above, can be interpreted from Fig. 13. It can be observed how different the actual temperature profile is from the temperature profile when the adiabatic-fin-tip is assumed. The slope of these curves in the Y direction gives the local heat flux along the fin and from the fin to the tubes. Consequently, if the slope of the curves is analyzed, it is easy to notice the deviation of the adiabatic-fin-tip assumption from the reality; the Fin2D solution presents a significant slope in the middle section of the fin whereas the adiabatic-fin-tip assumption imposes a null slope in the middle section. Fig. 13 shows that the solution temperature slope does not change its sign in any section along the fin height, which means that the fin receives heat from tube 2 and transfers heat to the tube 1 (and to the air). The slope for the cut fin changes its sign depending the fin root analyzed, hence the adiabatic-fin-tip assumption results in a wrong heat flux sign calculation (not only the absolute value) for the fin root of tube 1. The consequence of these differences is a large error in the heat capacity predicted for each tube and, therefore, in the refrigerant outlet properties.

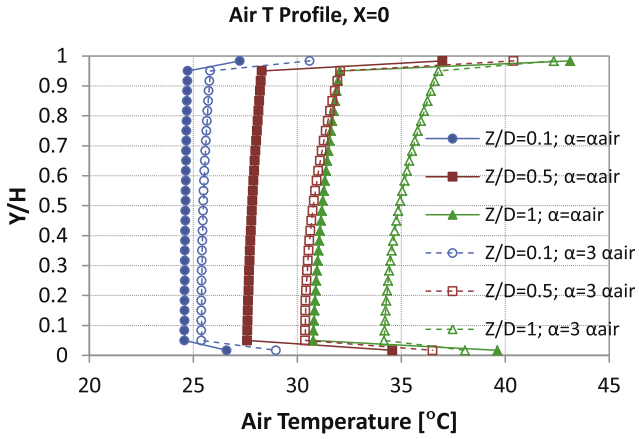

Fig. 14 – Air temperature profiles along the Y direction at the refrigerant inlet (X = 0) for three different locations along the Z direction when a difference temperature of 40 K exists between refrigerant inlets.

6.2.3. *Uniform air temperature along fin height*

To study the assumption of constant air temperature along the Y direction, Fig. 14 presents the corresponding air temperature profile in the same locations as those studied in Fig. 9, but now the studied scenario includes a 40 K temperature difference between refrigerant inlets.

The results shown in Fig. 14 are similar to those shown for Fig. 9 except two differences: the temperature difference between the air close to the tube and the rest of the air is now within 10 K, and the air temperature profile is less flat, particularly at the air outlet with the highest air-side heat transfer rate, due to the temperature difference between refrigerant inlets. This aspect is not accounted for by the fin theory, since it assumes a uniform air temperature. Although not studied here, an additional impact on the prediction results can be expected in an evaporator simulation due to the large temperature difference between the bulk air and the air close to the tube wall. In an evaporator model in the presence of dehumidification, the heat and mass transfer processes are strongly a function of local properties, which depend on the local temperatures.

7. Conclusions

A model for microchannel heat exchangers, Fin2D, accounting for heat conduction in all directions and in all heat exchanger elements was presented. The model allows for independent discretization for the refrigerant, tube and fins. The air has the same discretization as the fins. After verification against known analytical solutions, the model was employed to quantify prediction errors associated with

the classical ε-NTU modelling approach. Also, the classical assumptions were studied to evaluate their impact on the accuracy of simulation results. The following are the main conclusions of the study:

- The error obtained using the ε-NTU method depends on the ε-NTU relationship employed to calculate the effectiveness of each segment. For the studied case it is smaller than 3.5% for RMAU, smaller than 1% for BU and becomes larger as the air-side heat transfer coefficient increases. In general, the best option for the studied case is to use the tube-by-tube approach and to consider both fluids as unmixed although the effect of the mixed refrigerant assumption turned out negligible in the scenarios studied. However, this option can lead to larger errors when long length tubes are simulated because refrigerant properties and heat transfer coefficients can have significant variations, particularly when the refrigerant undergoes a phase change. It is not consistent to apply a segment-by-segment approach when the RMAU relationship is adopted.
- For the operating conditions studied, the impact of LHC effects along each direction in fins and tube walls, if considered separately, is not significant. The combined effect is more noticeable and may result in a capacity prediction error of as much as 2.5%, with the LHC_Z in the tube being the dominant effect. The impact of LHC depends on the air heat transfer coefficient.
- Using the adiabatic-fin-tip efficiency, which is commonly applied, leads to large errors in heat distribution per tube when a temperature difference between tubes exists. In addition, this assumption affects the global capacity prediction of gas coolers with large number of refrigerant passes. Thus, the fin cuts are justified in these heat exchanger topologies.
- The temperature of air close to the tube wall is very different than the bulk air temperature. This fact could have an important impact on local effects controlling the heat and mass transfer, e.g. dehumidification. It would have been interesting to evaluate the isolated effect of the non-uniform temperature profile of the air along the fin height.
- The developed model is able to capture most of the secondary heat transfer effects not taken into account by the classical ε-NTU approach or any model which applies the described classical assumptions; however, simulation of the 2D LHC problem in the wall requires a considerable computation time. The authors will continue working on a simplified model that will retain the most important effects. This will lead to much lower computation times while providing high accuracy of prediction of the complex heat transfer phenomena taking place in air-to-refrigerant microchannel heat exchangers.

Acknowledgements

Santiago Martínez-Ballester's work on this project was partially supported by Ministry for Education of Spain, under the training for university professors program (FPU).

REFERENCES

Asinari, P., Cecchinato, L., Fornasieri, E., 2004. Effects of thermal conduction in microchannel gas coolers for carbon dioxide. Int. J. Refrigeration 27 (6), 577–586.

Corberán J.M., Gonzálvez J., Montes P., Blasco R., 2002. 'ART' a computer code to assist the design of refrigeration and A/C equipment. International Refrigeration and Air Conditioning Conference at Purdue, IN, USA.

Corberán, J.M., De Cordoba, P.F., Gonzalvez, J., Alias, F., 2001. Semiexplicit method for wall temperature linked equations (SEWTLE): a general finite-volume technique for the calculation of complex heat exchangers. Numer. Heat Transfer, Part B. 40, 37–59.

Domanski, P.A., Choi, J.M., Payne, W.V., 2007. Longitudinal Heat Conduction in Finned-Tube Evaporator. 22nd IIR International Congress of Refrigeration, Beijing, China.

EVAP-COND, 2003. Simulation Models for Finned Tube Heat Exchangers. http://www.nist.gov/el/building_environment/evapcond_software.cfm.

Fronk, B.M., Garimella, S., 2011. Water-Coupled Carbon Dioxide Microchannel Gas Cooler for Heat Pump Water Heaters: Part II – Model Development and Validation. Int. J. Refrigeration 34, 17–28.

García-Cascales, J.R., Vera-García, F., Gonzálvez-Maciá, J., Corberán-Salvador, J.M., Johnson, M.W., Kohler, G.T., 2010. Compact heat exchangers modeling: condensation. Int. J. Refrigeration 33, 135–147.

Incropera, F.P., DeWitt, D.P., 1996. Fundamentals of Heat and Mass Transfer, fourth ed. John Wiley and Sons, New York.

Jiang, H.B., 2003. Ph. D. Thesis, Development of a Simulation and Optimization Tool for Heat Exchanger Design. University of Maryland, USA.

Jiang, H.B., Aute, V., Radermacher, R., 2006. Coildesigner: a general-purpose simulation and design tool for air-to-refrigerant heat exchangers. Int. J. Refrigeration 29 (4), 601–610.

Klein, S.A., 2004. Engineering Equation Solver. F-Chart Software, Madison, WI (USA).

Lee, J., Domanski, P.A., July 1997. Impact of Air and Refrigerant Maldistributions on the Performance of Finned-Tube Evaporators with R-22 and R-407C Report No.: DOE/CE/23810–81.

Lemmon, E.W., McLinden, M.O., Huber, M.L., 2002. REFPROP, Version 7.0. U.S. Department of Commerce, Maryland.

Park, C.Y., Hrnjak, P., 2007. Effect of Heat Conduction through the fins of a microchannel serpentine gas cooler of transcritical CO_2 system. Int. J. Refrigeration 30 (3), 389–397.

Patankar, S.V., 1980. Numerical Heat Transfer and Fluid Flow. Hemisphere, New York.

Shao, L.L., Yang, L., Zhang, C.L., Gu, B., 2009. Numerical modeling of serpentine microchannel condensers. Int. J. Refrigeration 32 (6), 1162–1172.

Singh, V., Aute, V., Radermacher, R., 2008. Numerical approach for modeling air-to-refrigerant fin-and-tube heat exchanger with tube-to-tube heat transfer. Int. J. Refrigeration 31 (8), 1414–1425.

Webb, R.L., 1994. Principles of Enhanced Heat Transfer. John Wiley and Sons, New York.

Yin, J.M., Bullard, C.W., Hrnjak, P.S., 2001. R-744 gas cooler model development and validation. Int. J. Refrigeration 24 (7), 692–701.

Zhao, Y., Ohadi, M.M., Radermacher, R., 2001. Microchannel Heat Exchangers with Carbon Dioxide Report No.: ARTI-21CR/10020–01.

Zilio, C., Cecchinato, L., Corradi, M., Schiochet, G., 2007. An assessment of heat transfer through fins in a fin-and-tube gas cooler for transcritical carbon dioxide cycles. HVAC&R Res. J. 13 (3), 457–469.